16th World Conference on Earthquake, 16WCEE 2017

Santiago Chile, January 9th to 13th 2017

Paper N° 4562

Registration Code: S-R1464625388

A NEW DESIGN PHILOSOPHY OF SEISMIC ANCHOR ELEMENTS FOR BRIDGES

C. Lüders[(1)], M. Criado[(2)]

[(1)] Professor Emeritus, Dept. of Structural and Geotechnical Engineering, Pontificia Universidad Católica de Chile, cluders@uc.cl
[(2)] MEng. Student, Dept. of Structural and Geotechnical Engineering, Pontificia Universidad Católica de Chile, mcriado1@uc.cl

Abstract

The seismic anchor elements of bridges are vertical steel bars that connect the slab of the superstructure with the bearing seat of the substructure. These bars are currently used on bridges in Chile and have the purpose of preventing the lifting of the superstructure during strong earthquakes. The Highways Manual and the New Seismic Design Criteria for Bridges of the Department of Public Works only specify the minimum strength they must have. They do not specify any prestress for them, no minimum or maximum distance between the anchor point to the bearing seat and anchorage point of them to the bridge deck, and no maximum or minimum length of these bars. In this paper the variables listed above, and the seismic behavior of bridges supported by elastomeric bearings that are fixed to the heel of the beams of the bridge, but can slip on the bearing seat, are analyzed. The elastomeric bearings are designed to be able to withstand the vertical loads of the bridge, the bridge temperature deformations and the maximum shear stress that can be generated in them because of the friction between the bearing seat and the elastomeric bearing. The support system is also designed so that the elastomeric bearing is able to accept temperature deformations of the bridge without sliding on the bearing seat. For strong earthquakes, the bearing slip on the bearing seat and seismic anchor elements provide restitution forces, to prevent span unseating and almost bring them back to its original position. Small permanent deformations after a strong earthquake may require a minor alignment of the superstructure. The friction between the elastomeric bearing and the bearing seat provides damping to the system. The proposed solution will improve the seismic performance and reduce the cost of the bridges because it decreases the stresses and strains in abutments and piers, as with a formal seismic isolation.

Keywords: Bridges; Seismic behavior; Seismic anchor cables; Elastomeric bearings.

1. Introduction

Seismic anchor bars of bridges are elements that were conceived in order to prevent the lifting of the superstructure of bridges as well as excessive horizontal displacement that could lead to the collapse of it. The Highways Manual of Department of Public Works (MOP, 2000) [1] proposes to use steel bars 22mm in diameter or larger, with specification ASTM A706M and ASTM A615M grade 280 and 420, designed to resist 50% of the weight of the bridge (100% after the 2010 Maule earthquake, according instructive "New Seismic Design Criteria for Bridges in Chile" [2]) multiplied by ground acceleration in the bridge site, expressed as a percentage of g. Meanwhile AASHTO LRFD Specifications (2012) [3] establish that anchoring devices must be provided to prevent the lifting of the deck in areas where the vertical seismic force is greater than, or equal to 50% of the permanent load. In neither case it considers lateral stiffness, or suggests any analysis procedure to evaluate its influence on the bridge behavior under seismic loads.

In 2010 Maule earthquake was evident that seismic bars did not have a suitable performance because of the absence of a structural design of these (Fig. 1). Such bars quickly attain yield stress and they offered no restriction to lateral movement of beams, which reached excessive displacements on the bearing seat that in several cases caused the collapse of the superstructure (Fig. 2). A detailed description of the damages of bridges during the Maule earthquake can be found, for example in studies by Elnashai et al. (2010) [4] and Kawashima et al. (2011) [5].

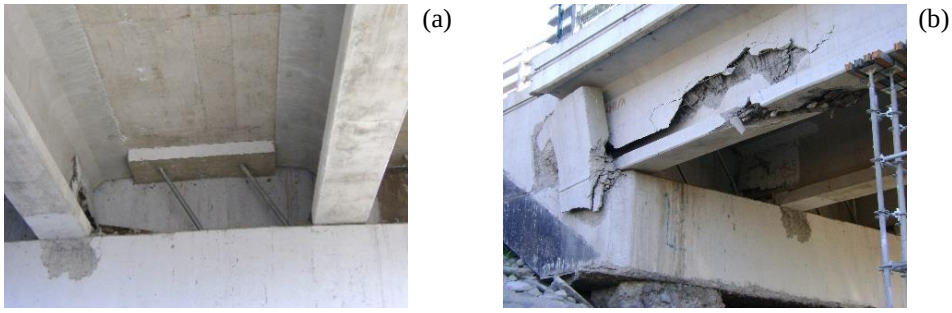

Fig. 1 – Damage in seismic anchor bars in Champa Bridge (Paine, Chile) during Maule earthquake of 27 February 2010 (by Carl Lüders)

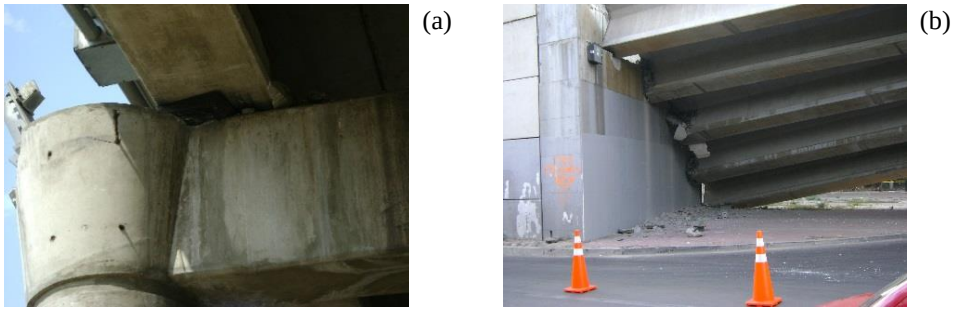

Fig. 2 –Americo Vespucio Norte Bridge (Santiago, Chile): (a) residual displacement, and (b) unseating of span, during Maule earthquake of 27 February 2010 (by Carl Lüders)

To understand the behavior of seismic bars under lateral loads it must take into account factors such as the type of seismic anchor (bar or cable), diameter and clear length of the element, the prestress level, the stiffness of elastomeric bearings, the friction between the bearing and substructure and other aspects that may influence the transverse behavior of the bridge.

In this paper the variables listed above are analyzed and a model with seismic pretensioned anchor cables for bridges supported by elastomeric bearings that are fixed to the heel of the beams, but can slip on the bearing seats, is proposed. The model considers elastomeric bearings designed to resist the vertical loads of the

superstructure, the bridge temperature deformations without sliding on the bearing seat and the maximum shear stress that can be generated in them because of the friction between the bearing seat and elastomeric bearing. The anchor cables will provide restitution forces necessary to avoid the bridge unseating and instead it attempts to return to its original position. The objective of this paper is to investigate the effect of anchor cables in reducing the seismic demand of bridges as with a formal seismic isolation, without replacing the elastomeric bearings by expensive seismic isolators.

2. Pretensioned seismic anchor cable model

2.1 Description of the proposed system

A system with pretensioned seismic anchor cables capable of generating, within the elastic range, restitution forces that allow controlling the maximum displacements of the bridge during strong earthquakes and limiting residual displacements to small values, is proposed.

The system consists of a pretensioned cable with section A, modulus of elasticity E and initial length equal to $(L_1 + L_2)$ which is connected in series with a spring (stiffness K_o and natural lenght l_o) between the bridge deck and bearing seat. The cable passes through the diaphragm. The ratio of the height of the diaphragm and the distance between the bridge deck and the bearing seat can regulate the effectiveness of the proposed system as a restitution element of the bridge. During the assembly, spring and cable are tensioned with a force T_o. The spring can be materialized by a piece of cable without bonding in a duct within the pier or abutment.

For analysis it can identify two cable segments hereinafter indicated as "section 1" (defined as the portion of the cable within the diaphragm) and "section 2" (defined as the free portion of the cable). In Fig. 3(a) the geometry of the proposed system in its undeformed shape, is shown, where l_0 is the initial length of the spring (without tension), h_1 is the height of the diaphragm and h_2 is the clear distance between diaphragm and bearing seat. Fig. 3(b) shows pretensioned anchor cable, where δ_{so} and δ_{co} are the elongation due to prestressing force of the spring and cable, respectively. Fig. 3(c) shows the anchoring system with the diaphragm laterally displaced in Δ_h, where L_1 and L_2 correspond to the natural lengths of the cable in sections 1 and 2, respectively, δ_s is the spring deformation, and δ_1 and δ_2 are the deformations of cable in sections 1 and 2, respectively.

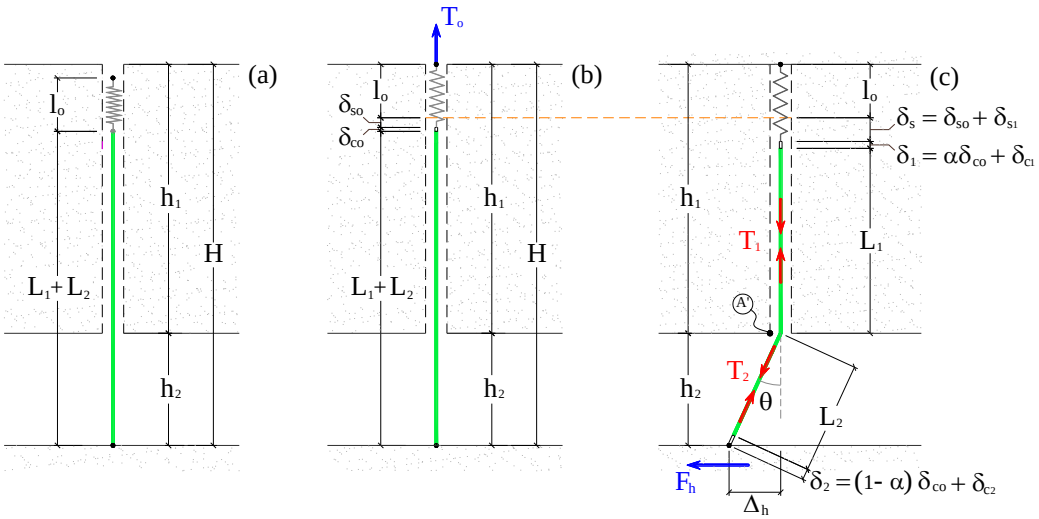

Fig. 3 – Scheme of proposed model: (a) Initial position without prestress, (b) Initial position with prestress, (c) Deformed shape

If a horizontal displacement Δ_h on bridge deck is imposed, slip of the cable at point A' in Fig. 3(c) will occur when:

$$T_1 = T_2 e^{-\mu\theta} \tag{1}$$

where μ corresponds to the friction coefficient at point A', and θ is the deflection angle in radians between section 1 and section 2 of the anchor cable. The above expression implies a change of magnitude in L_1 and L_2 lengths during the bridge movement regarding the substructure. Only the sum $L_1 + L_2$ will remain constant and equal to the initial length of the cable.

Eq. (1) is satisfied when cable slips at point A' with increasing bridge displacements. When the movement changes direction cable slip at point A' does not occur immediately. Initially, only the cable section 2 recovers elastically. When T_2 reaches the value given in Eq. (2), slip at point A' will start, and cable section 1 will start recovering.

$$T_2 = T_1 e^{-\mu\theta} \tag{2}$$

In Eq. (1) and Eq. (2), T_1 and T_2 are the forces on the anchor cable in sections 1 and 2, respectively:

$$T_1 = K_1\delta_1\,, \quad T_2 = K_2\delta_2 \tag{3) , (4}$$

where K_1 and K_2 are cable stiffness in sections 1 and 2, respectively, and they are given by:

$$K_1 = \frac{AE}{L_1}\,, \quad K_2 = \frac{AE}{L_2} \tag{5) , (6}$$

The spring force is given by:

$$T_1 = K_o\delta_s \tag{7}$$

Initial deformations due to prestressing force T_o in cable and spring are, respectively:

$$\delta_{co} = \frac{T_o(L_1 + L_2)}{AE}\,, \quad \delta_{so} = \frac{T_o}{K_o} \tag{8) , (9}$$

The total deformation of anchor cable in sections 1 and 2 are, respectively:

$$\delta_1 = \alpha\delta_{co} + \delta_{c1}\,, \quad \delta_2 = (1-\alpha)\delta_{co} + \delta_{c2} \tag{10) , (11}$$

where δ_{c1} and δ_{c2} are deformations in sections 1 and 2 of anchor cable due to horizontal displacement Δ_h:

$$\delta_{c1} = \frac{(T_1 - T_o)L_1}{AE}\,, \quad \delta_{c2} = \frac{(T_2 - T_o)L_2}{AE} \tag{12) , (13}$$

The total deformation of the spring is defined as:

$$\delta_s = \delta_{so} + \delta_{s1} \tag{14}$$

where δ_{s1} is the spring deformation due to horizontal displacement Δ_h:

$$\delta_{s1} = \frac{(T_1 - T_o)}{K_o} \tag{15}$$

Finally, the horizontal force produced by displacement Δ_h is given by:

$$F_h = T_2\, sin\,\theta \tag{16}$$

2.2 Constitutive model of a particular seismic anchor cable system

In order to obtain a constitutive relation of a particular system anchor cable, the geometry in Fig. 4 is considered, which consists in a superstructure with diaphragms high h_1=1.65m and clear distance between diaphragm and bearing seat h_2=0.45m. The parameters listed in Table 1 for anchoring system were assumed.

Table 1 – Constitutive model parameters for seismic anchor cable

A (mm^2)	E (MPa)	F_{py} (MPa)	P_y (kN)	T_0 (kN)	K_o (kN/mm)	μ	l_o (m)	L_1+L_2 (m)	δ_{so} (mm)	δ_{co} (mm)
139	210000	1674	233	47	4.38	0.5	0.30	1.787	10.65	2.85

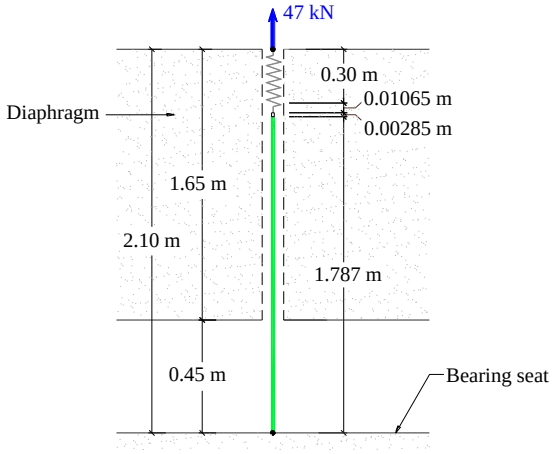

Fig. 4 – Geometry of seismic anchor system

Solving the problem for T_1 and T_2, and considering a displacement Δ_h increasing in one direction, the relationships T_2 vs Δ_h, and F_h vs Δ_h for the anchor cable system is obtained. In Fig. 5(a) the axial tension in the free portion of the cable as a function of the horizontal displacement, are shown. It is observed that system starts with initial force of T_0=47kN and then it describes a non-linear behavior until it reaches the yield strength equal to 233kN for a horizontal displacement equal to 0.1965m.

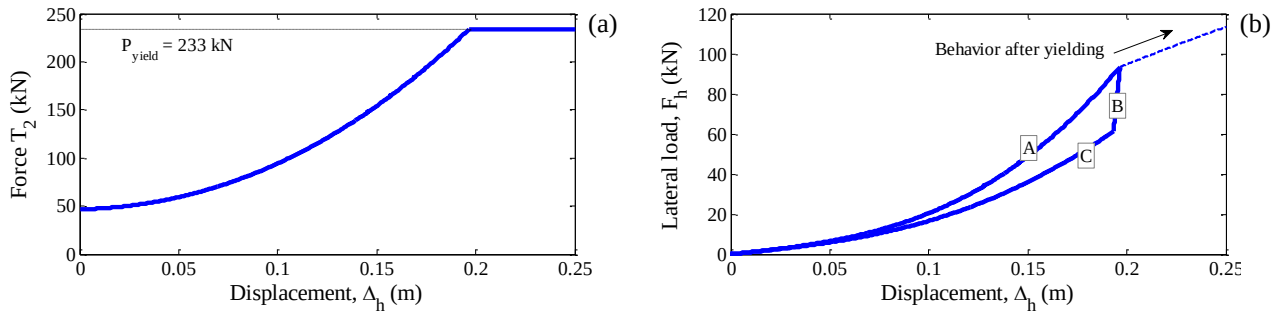

Fig. 5 – Constitutive model of seismic anchor cable: (a) T_2 vs Δ_h, (b) F_h vs Δ_h

Fig. 5(b) shows the F_h vs Δ_h relationship and represents the constitutive model of pretensioned anchor cable system. The curve "A" corresponds to loading phase of system in the positive direction, wherein both 1 and 2 cable sections are deformed. The segment "B" represents the unloading starting. In this region there is no slip, only an elastic recovery occurs in the cable section 2. In curve "C" an inversion in the direction of frictional forces take place and cable starts to slip relative to point A'. The system returns to initial state when Δ_h=0, and has not exceeded yielding in phase A. It is noted that under small displacements the system is very flexible. As

displacement increases, the system has greater lateral stiffness. In turn, the system is slightly rigid during loading phase and more flexible during unloading.

In order to compare the lateral stiffness of proposed system against the model stablished in the Highways Manual (MOP), it is considered the geometry of Fig. 4 eliminating the spring length l_0 and prestressing force T_o, so that h_1 =1.65m and h_2=0.45m. In this case the system consists in bars Grade 420 ϕ_s=22mm in diameter. Thus, A=380mm^2, F_y=420MPa and P_y=160kN; a friction coefficient μ=0.5 is assumed. The force-deformation in Fig. 6 reveals that seismic bars reach the yield stress at very low displacements so they do not provide sufficient transverse stiffness to seismic loads.

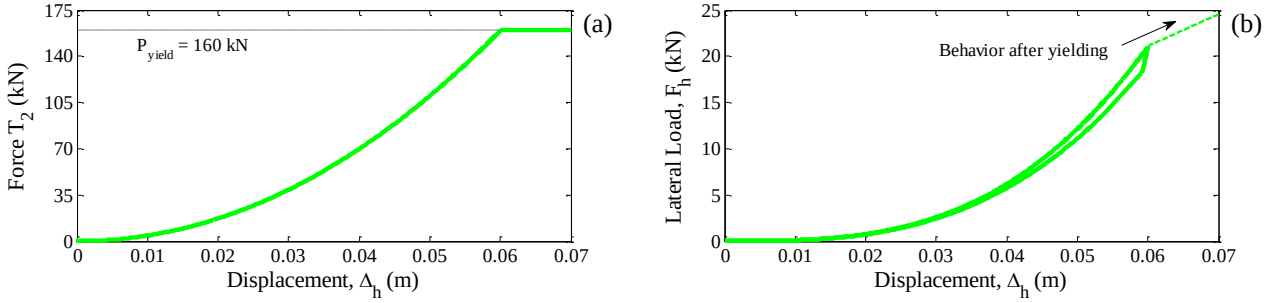

Fig. 6 – Constitutive model of seismic bars according to MOP: (a) T_2 vs Δ_h, (b) F_h vs Δ_h

This fact is supported by research conducted by A. Martinez [6], who tested three specimens consisting in concrete elements to represent the diaphragm and the bearing seat, connected by two seismic bars. Each specimen was subjected to displacement cycles between 1mm and 150mm of amplitude. In all cases the bars reached yielding to displacements below 70mm, concluding that seismic bars proposed by MOP offer no restriction to horizontal displacement of the superstructure.

Fig. 7 illustrates the advantage of anchor cable proposed system over ordinary steel bars system by MOP, reflected in a considerable increment in the restitution force and the maximum displacement tolerated before yielding occurs.

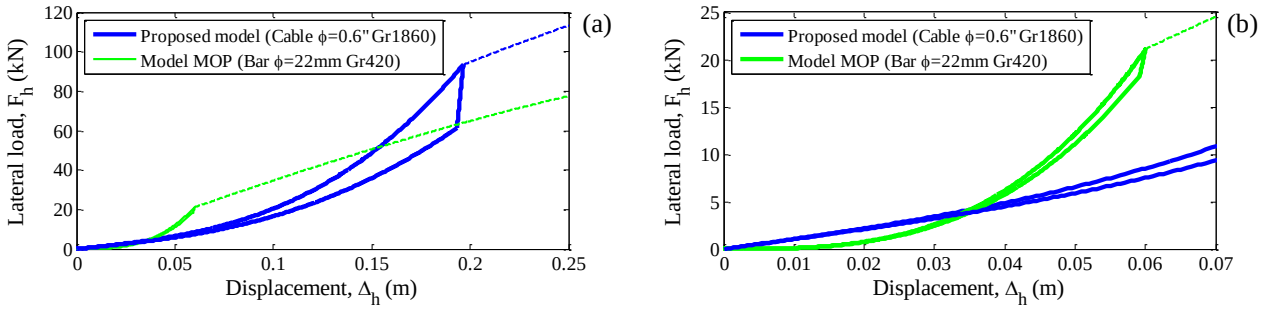

Fig. 7 – Comparison between system required by MOP and anchor cable proposed model: (a) Overview of response curves, (b) Zoom of left portion of curves.

The main factors that determine these differences are the cable strength over ordinary steel bars, the prestressing force and the spring flexibility, as shown in Fig. 8. The high cable strength and spring flexibility allow the superstructure reaches large deformations before the cable yields. Prestress introduces an additional restitution force that limits the residual displacements. On the other hand, a greater cable length in its free portion increases the magnitude of displacement before the anchoring system can develop significant restitution forces.

Fig 8(a) shows the variation of spring stiffness for h_2/H=0.20 relationship and Fig 8(b) indicates the effect of h_2/H relationship for spring stiffness equal to 20% of cable section 1 stiffness.

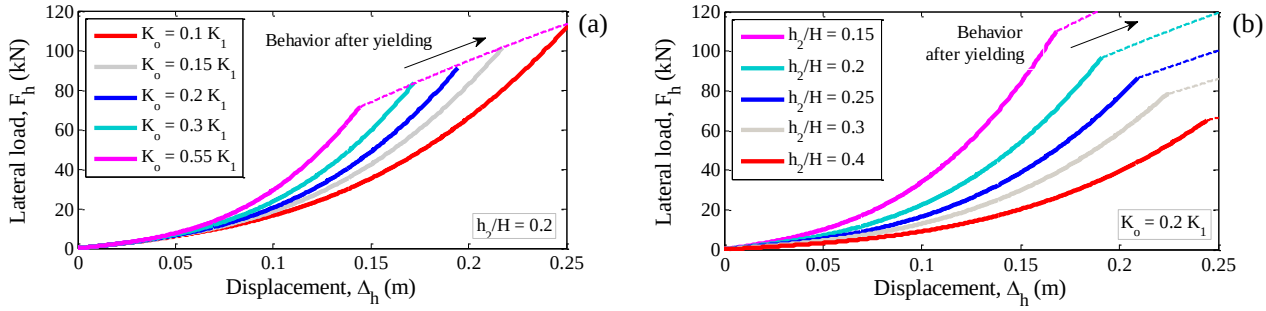

Fig. 8 – Factors affecting anchor cable system: (a) Spring stiffness, (b) h_2/H relationship.

3. Elastomeric bearings

3.1 Behavior of elastomeric bearings under cyclic shear loading

The elastomeric bearings are designed as elements to resist the vertical loads and accommodate translational and rotational movements of the bridge. Several studies have analyzed the bearings behavior under shear stresses, concluding that they provide stable hysteretic behavior with large energy dissipation.

Steelman et al. (2013) [7] investigated the slip response of laminated elastomeric bearings under shear stresses. For this purpose a set of specimens were subjected to shear strains between 25% and 400% of total thickness of elastomer. Tested bearings exhibited an approximately linear elastic behavior until the moment which the bearing slip starts. Slip initiating was directly proportional to the axial load and occurred for shear deformations between 125% and 250% of elastomer height. Rubilar (2015) [8] studied nonlinear behavior of elastomeric bearings under seismic loads. They used specimens with typical configurations of elastomeric bearings used in chilean bridges which were subjected to displacements on the order of 25% to 160% elastomer height with similar results to those of Steelman et al.

Both Steelman et al. (2013) and Rubilar (2015) demonstrated that elastomeric bearings have an approximately elastic linear behavior before sliding occurs. To overcome friction a peak is originated because of the change in friction coefficient of static to dynamic and the bearing begins to slip on the substructure maintaining approximately constant force, as shown in Fig. 9. For small deformations bearings exhibit a linear behavior and then, to overcome the friction force, the load is stabilized, so that if the peaks at the start of slip are ignored, it can be assumed an elastoplastic behavior of the bearing.

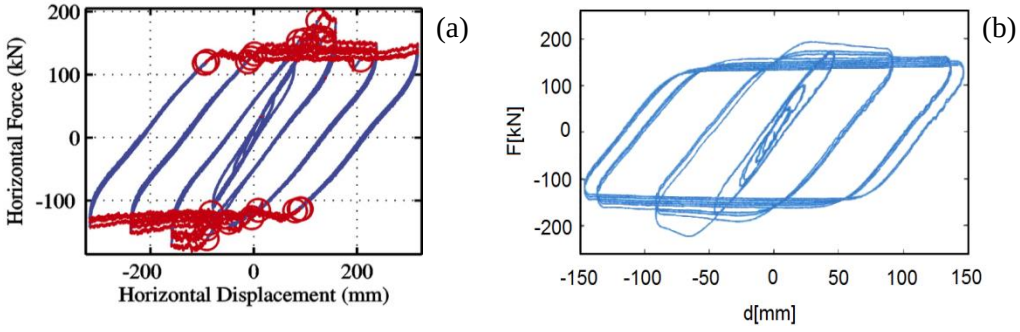

Fig. 9 - Experimental model of elastomeric bearings for cyclic stresses: (a) Steelman et al. (2013) [7], (b) Rubilar (2015) [8]

3.2 Constitutive model of elastomeric bearings

For the particular example being analyzed, the elastomeric bearings properties in Table 2 are considered. The vertical load on each bearing is N=550kN, the friction force which slip is initiated with, is $F_r=\mu_s N$=275kN, that produces the maximum deformation $\delta_{b\,max}$=55.9mm corresponding to 80% of elastomer height. Assuming a perfect elastoplastic behavior, the F_h vs Δ_h relationship of the elastomeric bearing is shown in Fig.10.

Table 2 – Constitutive model parameters for elastomeric bearing.

μ_s	h_r (mm)	L (mm)	W (mm)	A (mm^2)	N (kN)	F_r (kN)	G (MPa)	$\delta_{b\,max}$ (mm)	K_b (kN/mm)
0.5	70	600	450	2700	550	275	1.3	55.9	4.92

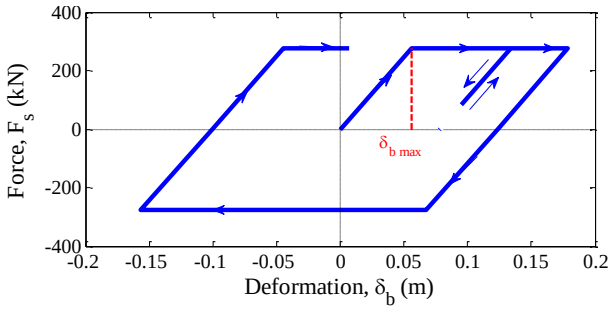

Fig. 10 – Constitutive model of elastomeric bearing

4. Constitutive model of elastomeric bearing + pretensioned anchor cable system

This model is obtained by superimposing the behavior in Fig. 5(b) with Fig. 10. As a result, the behavior shown in Fig. 11(b) is obtained. This model follows a substantially linear path until the maximum deformation of the elastomer, $\delta_{b\,max}$. Thereafter, the bearing slips on the substructure and takes the nonlinear characteristic curve of anchor cable.

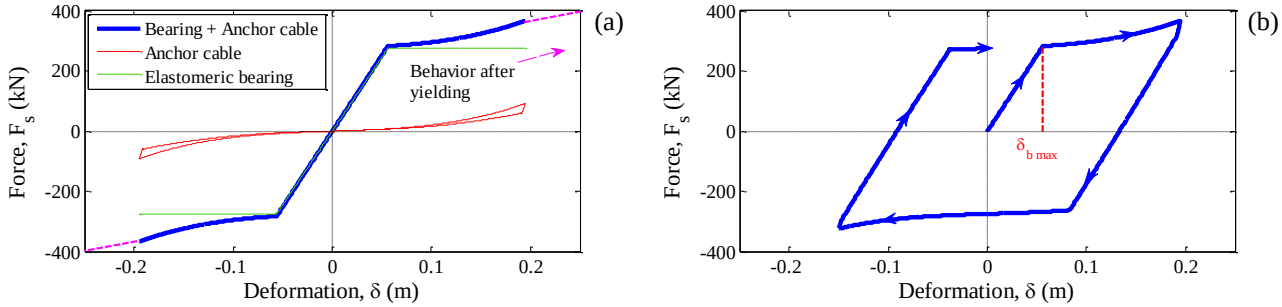

Fig. 11 – Constitutive model of elastomeric bearing and pretensioned anchor cable system

5. Evaluation of the seismic response

In order to evaluate the efficiency of the proposed system, the seismic response of three different models were analyzed: fixed bearing, unbonded bearing and unbonded bearing with seismic anchor cable. In each case, a single degree of freedom system (SDOF) was modeled and it was subjected to the "Constitucion" record of 2010 Maule earthquake [9] which is shown in Fig. 12, with a peak ground acceleration (PGA) equal to 0.63g. A

Nonlinear Time History analysis was made by the Newmark's method of average acceleration [10] using the Matlab R2013a software [11], except for the fixed bearing system, in which case the linear method was used.

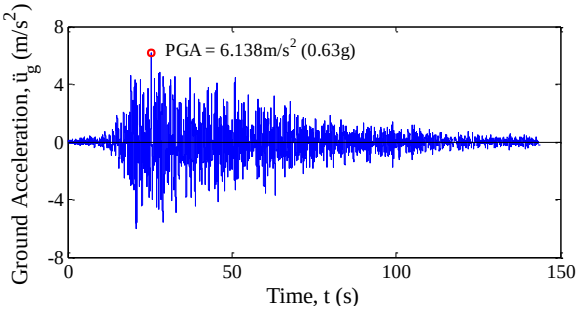

Fig. 12 – "Constitucion" Record, Maule Earthquake 2010

5.1 Case 1: Fixed elastomeric bearing

The system consists of an elastomeric bearing anchored to the beam and the substructure with the characteristics indicated in Table 2. Considering a SDOF system with a linear stiffness K_b =4.92 kN/mm, the period is calculated as $T = 2\pi\sqrt{m/K_b} = 0.67$s. In this case a fully elastic behavior is assumed, as shown in Fig. 13(b). The maximum displacement response is 0.313m (Fig. 13(c)), value 4.5 times higher than the total thickness of the elastomer and it can hardly be reached without fails in shear. Moreover, the maximum acceleration response is equal 28.31m/s^2 (Fig. 13(d)) equivalent to 2.9g, which introduces a significant shear to substructure.

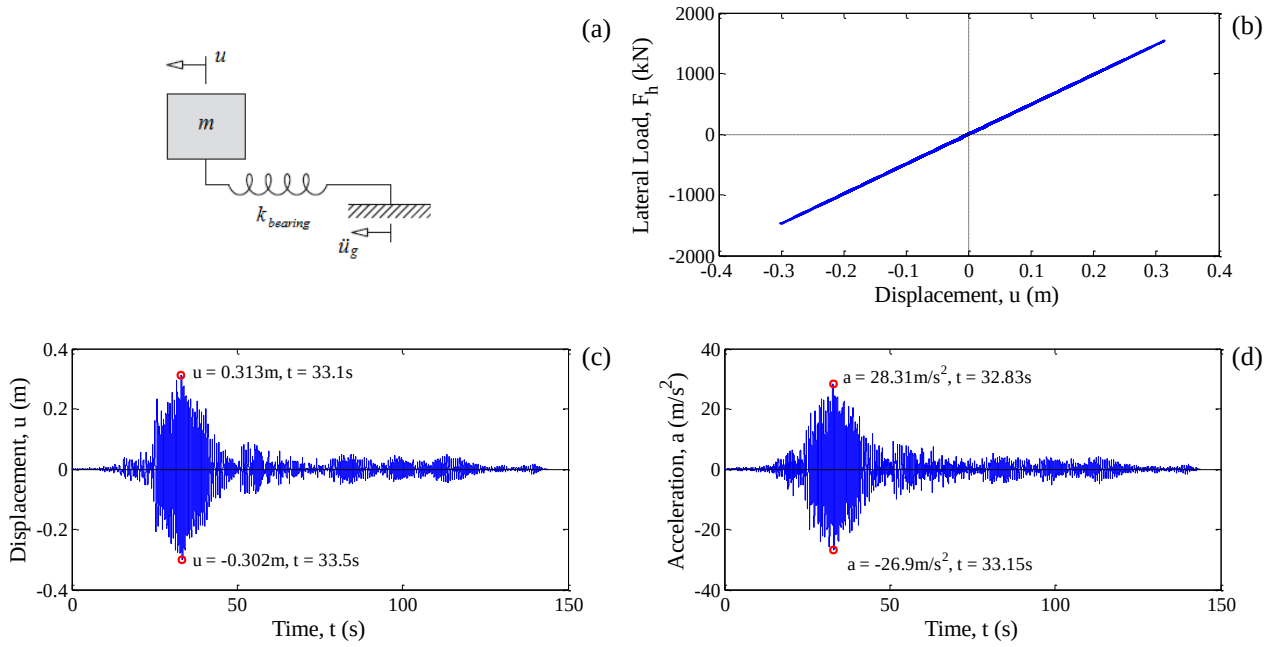

Fig. 13 – Fixed elastomeric bearing: (a) SDOF Model, (b) F_h vs Δ_h relationship, (c) Displacement response, (d) Acceleration response

5.2 Case 2: Unbonded elastomeric bearing

In this case the elastomeric bearing was considered connected at its top surface to the heel of the beam but is not anchored at its base at the substructure. So, slip will start when the shear stress exceeds the friction force F_r=275kN. The period is the same as in the previous case equal to T =0.67s. The system stiffness is according to the model of Fig. 10. The results show that when system reaches the friction force, the bearing slips on the substructure until a displacement equal to 0.241m. If the elastomeric bearing was not fixed to the heel of the beam, it could move along the bearing seat, to be removed completely and fall, as happened in several cases during the 2010 Maule earthquake (Fig. 2). Around 50 seconds the slip of the system on the bearing seat ends, and only the elastomer deforms elastically. After the excitation, bearing remains displaced approximately 0.13m from its original position as seen in Fig. 14(c). The maximum acceleration demand in this system is much lower compared with case 1, with a value equal to 9.84m/s^2 (Fig. 14(d)) equivalent to approximately 1g.

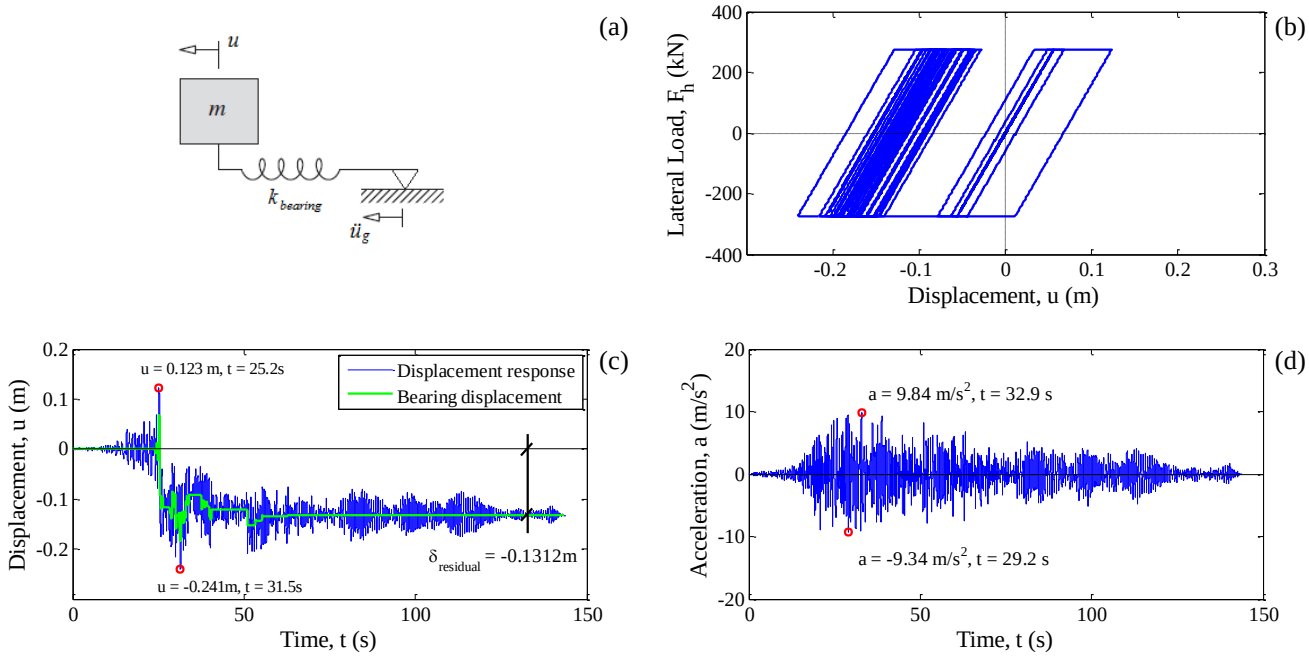

Fig. 14 – Unbonded elastomeric bearing: (a) SDOF Model, (b) F_h vs Δ_h relationship, (c) Displacement response, (d) Acceleration response

5.3 Case 3: Unbonded bearing + pretensioned anchor cable system

This system consists of an elastomeric bearing with the same properties of the previous case, anchored to the beam only, and connected in parallel with the pretensioned anchor cable proposed. The stiffness corresponds to the non-linear model of Fig. 11(b). Here the system is slightly more rigid than in the previous case. The pretensioned cable attached to the spring K_o adds a system restitution force which tends to return the bridge superstructure to its original position thereby reducing permanent deformation. When the friction force is overcame, structure slips a maximum displacement of 0.172m (Fig. 15(c)) and at the end of the excitation residual displacement is approximately 0.03m, which is very close to its original position. The acceleration demand for this case is 10.1m/s^2 (Fig. 15(d)) corresponding to 1.03g, is slightly larger than in the unbonded case (1g), but much lower than in the system with fixed bearings (2.9g).

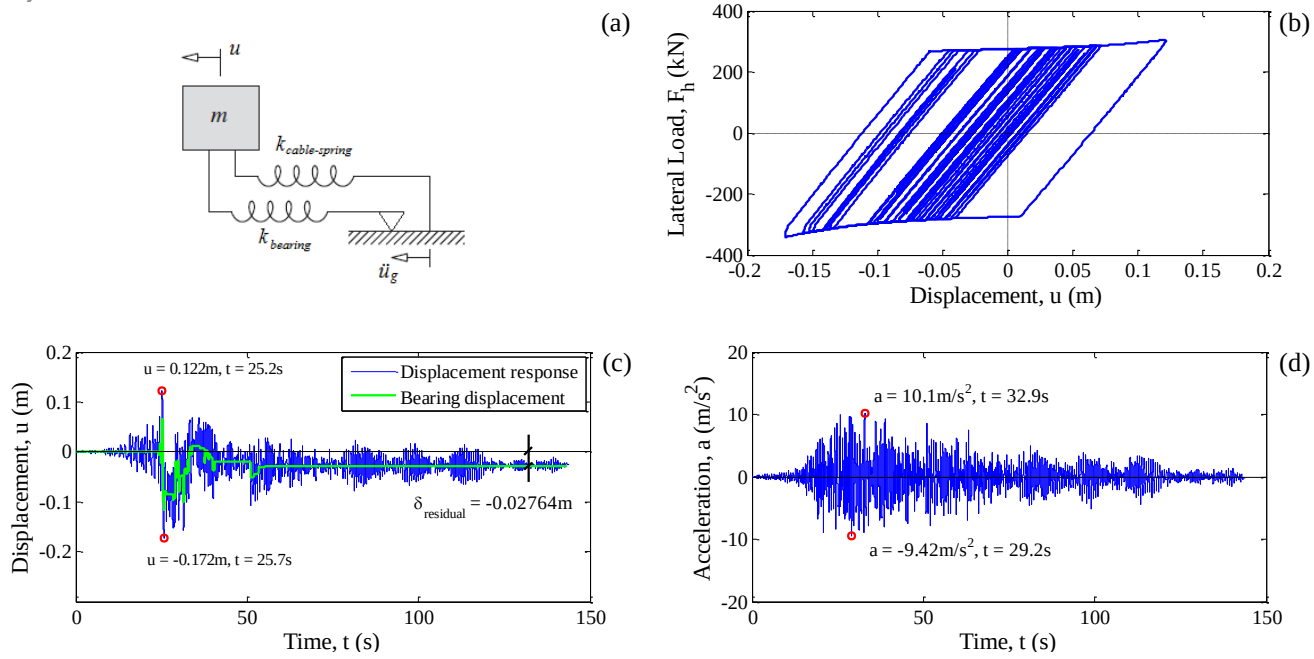

Fig. 15 – Unbonded bearing + pretensioned anchor cable: (a) SDOF Model, (b) F_h vs Δ_h relationship, (c) Displacement response, (d) Acceleration response

6. Results and Discussion

According to the document "New Seismic Design Criteria for Bridges in Chile", MOP requires anchoring of bearing plates to beams and substructure, giving preference to the use of seismic isolators. Thus when analyzing the case 1, the high demands of displacement and base shear obligate to implement a seismic isolation system, if it were otherwise the movement restriction stablish by MOP in traditional bearing systems would produce early shearing failure of the bearing. Shear deformations in bearings fixed to the beam and the bearing seat (case 1) is nearly triple the deformations experienced by the bearings which can freely slip (cases 2 and 3). In alternatives 2 and 3 the maximum shear deformations experienced by elastomeric bearings are very similar. The drawback in alternative 2 is that permanent displacements on the bridge are very large.

Case 3 represents the most attractive alternative since the restitution force of the pretensioned anchor cable system limits the permanent displacement of the superstructure and returns it approximately to its initial position. This advantage over Case 2 is clearly seen by comparing Fig. 14(c) with Fig. 15(c). Is noted for the example studied, a reduction of almost 80% of the residual displacement by including the pretensioned anchor cable compared to the system which elastomeric bearing is permitted to slide on the bearing seat.

7. Conclusions

This paper proposes and analyzes an efficient alternative for anchoring bridges supported by elastomeric bearings designed to accept in elastic range temperature deformations. The bearings are not fixed to the bridge substructure (bearing seat), so that during strong motions they can slip on the bearing seat. This fact limits the shear stresses induced in the bearings during strong earthquakes and provides damping to the system. A system with anchor cable produces a restitution force that returns the bridge deck almost to its initial position at the end of an intense earthquake.

In order to appreciate the advantages of the proposed system were analyzed three cases. Case 1: elastomeric bearing fixed to the beam and bearing seat; Case 2: elastomeric bearing fixed to the beam and free respect to the substructure; Case 3: elastomeric bearing fixed to the beam and free respect to the substructure, in

conjunction with pretensioned anchor cable. Each case was modeled as a SDOF and the seismic behavior of the bridge was studied. It was observed that case 1 induces large shear stresses in the elastomeric bearing that obligate to replace it by seismic isolators with the increased cost associated. In case 2 slipping of the bearing on the substructure provides energy dissipation, and the response in terms of displacement and acceleration is significantly reduced compared to the case 1. Its main drawback is the lack of control of the displacements of the bridge that can lead to the collapse of the superstructure as happened in several cases during the 2010 Maule earthquake. Case 3 that adds to the previous case an anchoring system with pretensioned anchor cable-spring, limits these displacements; base shear demand is similar to the case 2 and the shear demand of elastomeric bearings remains in the elastic range of them. Placing a small friction interface between the elastomeric bearing and the bearing seat may further enhance the effectiveness of the proposed system.

The pretensioned seismic anchor cable system provides a similar performance to a classic isolation but at a significantly lower cost. It is important that future research include experimental studies to validate the model proposed here.

8. References

[1] MOP, (2000): Manual de Carreteras, Instrucciones y Criterios de Diseño. *Dirección de Vialidad, Ministerio de Obras Públicas*, Chile.

[2] MOP, (2011): Nuevos criterios sísmicos para el diseño sísmico de puentes en Chile. *Dirección de Vialidad, Ministerio de Obras Públicas*, Chile.

[3] AASHTO (2012): Standard Specifications for Highway Bridges. *American Association of State and Highway Transportation Officials*, Washington, D.C.

[4] Elnashai A. S., Gencturk B., Kwon O-S, Al-Qadi I. L., Hashash Y., Roesler J. R., Kim S. J., Jeong S-H., Dukes J., Valdivia A., (2010): The Maule (Chile) Earthquake of February 27, 2010: Consequence assessment and case studies. *MAE Center Report No. 10-04*.

[5] Kawashima K., Unjoh S., Hoshikuma J-I., Kosa K., (2011): Damage of bridges due to the 2010 Maule, Chile, Earthquake. *Journal of Earthquake Engineering 2011/15*.

[6] Martínez, A. (2015): Efecto de las barras sísmicas en el comportamiento sísmico transversal de puentes de hormigón armado. *M.S. Thesis, Pontificia Universidad Católica de Chile*, Chile.

[7] Steelman, J. S., Fahnestock, L. A., Filipov, E. T., LaFave, J. M., Hajjar, J. F., Foutch, D. A. (2013): Shear and friction response of nonseismic laminated elastomeric bridge bearings subject to seismic demands. *Journal of Bridge Engineering* ASCE *2013/07*, American Society of Civil Engineers.

[8] Rubilar, F. (2015): Modelo no lineal para predecir la respuesta sísmica de pasos superiores. *M.S. Thesis, Pontificia Universidad Católica de Chile*, Chile.

[9] Red de Cobertura Nacional de Acelerógrafos, RENADIC, (2010): Terremoto del Maule de Febrero 27, 2010 Mw=8.8. *Departamento de Ingeniería Civil, Universidad de Chile*, Chile.

[10] Chopra, Anil K. (2012): *Dynamics of Structures*. Pearson, 4nd edition.

[11] The Mathworks, Inc. (2010): MATLAB R2010a.